

# Automated detection of heart ailments from 12-lead ECG using complex wavelet sub-band bi-spectrum features

Rajesh Kumar Tripathy , Samarendra Dandapat

Department of Electronics and Electrical Engineering, Indian Institute of Technology Guwahati, Guwahati 781039, India

✉ E-mail: rajeshiitg13@gmail.com

Published in Healthcare Technology Letters; Received on 1st November 2016; Revised on 16th January 2017; Accepted on 18th January 2017

The complex wavelet sub-band bi-spectrum (CWSB) features are proposed for detection and classification of myocardial infarction (MI), heart muscle disease (HMD) and bundle branch block (BBB) from 12-lead ECG. The dual tree CW transform of 12-lead ECG produces CW coefficients at different sub-bands. The higher-order CW analysis is used for evaluation of CWSB. The mean of the absolute value of CWSB, and the number of negative phase angle and the number of positive phase angle features from the phase of CWSB of 12-lead ECG are evaluated. Extreme learning machine and support vector machine (SVM) classifiers are used to evaluate the performance of CWSB features. Experimental results show that the proposed CWSB features of 12-lead ECG and the SVM classifier are successful for classification of various heart pathologies. The individual accuracy values for MI, HMD and BBB classes are obtained as 98.37, 97.39 and 96.40%, respectively, using SVM classifier and radial basis function kernel function. A comparison has also been made with existing 12-lead ECG-based cardiac disease detection techniques.

**1. Introduction:** Life-threatening cardiac ailments occur due to improper conduction [bundle branch block (BBB)], obstruction in one of the coronary arteries [myocardial infarction (MI)] and abnormal heart muscle [hypertrophic cardiomyopathy (CM)] [1]. Multilead or 12-lead ECG is commonly used for detection of MI, BBB and hypertrophic CM [1–3]. Automated detection of heart ailments is an active area of research in cardiovascular signal processing [4]. The automated diagnostic system (ADS) consists of ECG data, preprocessing, feature extraction and classification [5, 6]. The key component of an ADS is the evaluation of features from the ECG signal [7]. In ADS, both direct and indirect methods are used for computing the diagnostic features of ECG. The direct method is based on the evaluation of morphological features such as the amplitude, the duration and the shape of the clinical components (P-wave, QRS-complex and T-wave) of ECG. The indirect method uses different signal processing techniques for evaluation of diagnostic features.

In the literature, several feature extraction methods have been reported for the detection of cardiac disorders such as MI, BBB and heart muscle disease (HMD) from 12-lead ECG signals. The methods are based on continuous wavelet transform [8], polynomial curve fitting [9], hermite polynomials [10], multivariate multiscale sample entropy [11], random projection [12] and tensor discriminant analysis [13]. Some of the methods have used various morphological features of 12-lead ECG for detection of cardiac disorders [14, 15]. For evaluation of these morphological features, it is required to detect the P, Q, R, S, T points of each ECG lead. The 12-lead ECG-based reported methods are also based on the detection of single pathology [either heart ailments (MI or CM) or normal sinus rhythm (NSR)]. In intensive care unit, the cardiologists examine the defect in the conduction process of the heart, the occlusion in the coronary arteries of the heart and the heart muscle defects from the 12-lead ECG recordings [5]. Therefore, a method based on the automated detection and classification of BBB, HMD and MI pathology will be helpful to assist the cardiologist for providing better diagnostic decision.

In [16], the multiscale energy and eigenspace (MEES) features of multilead ECG have been proposed for the detection and localisation of MI. The MEES features are evaluated using discrete wavelet transform (DWT) of 12-lead ECG. The dual tree complex wavelet transform (DTCWT) overcomes the drawbacks of DWT and it

has been used for various ECG processing applications [17–19]. In addition to magnitude information, the DTCWT of ECG also provides the phase information at different scales. In our previous study, the multiscale phase alternation (PA) features have been proposed for analysis of 12-lead ECG during HMD, BBB and MI pathologies [20]. Although, the multiscale PA features of 12-lead ECG are effective for detection of MI, they fail to capture the pathological changes during BBB and HMD. Hence, further investigation into the features from the CW coefficients of 12-lead ECG is required for accurate detection of life-threatening cardiac ailments.

The higher-order spectra (HOS) have been widely used in the analysis of bio-medical signals [21–23]. The HOS measures the deviation from the Gaussianity, the phase correlation, the magnitude correlation and the nonlinearity of a time-series data. The wavelet-based HO spectral (WHOS) features have been used for tonic pain characterisation from electroencephalogram (EEG) signal [24]. The WHOS features of EEG are evaluated using the HOS and discrete time continuous wavelet transform. The CW coefficients at different sub-bands are calculated using the DTCWT-based processing of ECG [19, 20]. These CW coefficients capture the grossly divided morphological components of ECG signal. The CW sub-band bi-spectrum (CWSB) of 12-lead ECG can be evaluated using the higher-order CW analysis (HOCWA). The higher-order magnitude and phase correlations of the CW coefficients of 12-lead ECG are captured using the CWSB. The structure of the CWSB matrices of 12-lead ECG will be different for NSR and for various cardiac ailments. It is expected that the features evaluated from the CWSB of 12-lead ECG will be helpful for detection of cardiac ailments. In this work, the CWSB features of 12-lead ECG are proposed. These features are used for detection of MI, HMD and BBB. The rest of this Letter is arranged as follows. In Section 2, the proposed CWSB features of 12-lead ECG using HOCWA is presented. The detection of cardiac ailments using the CWSB features is described in Section 3. The results and the discussion are presented in Section 4 and the conclusions of this Letter are written in Section 5.

**2. Proposed CWSB features:** The proposed CWSB features are evaluated using three steps: namely, the DTCWT of 12-lead ECG, the HOCWA and the calculation of magnitude and phase features of CW bi-spectrum of significant sub-bands.

2.1. DTCWT of 12-lead ECG: The DTCWT uses a pair of filter banks to evaluate CW coefficients of an ECG signal at different sub-bands [17]. For a 12-lead ECG signal  $x^m(n)$ , the CW coefficients of each ECG lead at different sub-bands are evaluated. The approximation sub-band and the  $l$ th detail sub-band ( $l = 1, 2, \dots, L$ ) CW coefficients for the  $m$ th ECG lead are given as [20]

$$cA_L^m(k) = \tilde{c}A_L^m(k) + j\overline{c}A_L^m(k) \quad (1)$$

$$cD_l^m(k) = \tilde{c}D_l^m(k) + j\overline{c}D_l^m(k) \quad (2)$$

In this work, the significant sub-bands of 12-lead ECG are selected based on the CW energy each sub-band. Figs. 1a and b depict the variation of average CWE of all ECG leads with number of sub-bands at decomposition levels of  $L = 6$  and  $7$  for NSR, MI, BBB and HMD cases. It is observed that for six-levels DTCWT-based decomposition of 12-lead ECG, the  $cA_6$ ,  $cD_6$ ,  $cD_5$  and  $cD_4$  sub-bands have higher-energy values than other sub-bands. These four significant sub-bands are considered for HOCWA.

2.2. Higher-order complex wavelet analysis: The HOCWA is based on the evaluation of CW bi-spectrum of 12-lead ECG at different sub-bands. In this Letter, the CW bi-spectrum is evaluated for diagnostically significant sub-bands. The CW coefficients of multilead ECG are given by,  $s^m(k) = \tilde{s}^m(k) + j\overline{s}^m(k)$ , where  $s$  is the significant sub-bands of each ECG lead. For  $L = 6$  and  $7$ , the significant sub-bands are  $s \in (cA_6, cD_6, cD_5, cD_4)$  and  $s \in (cA_7, cD_7, cD_6, cD_5, cD_4)$ , respectively. The bi-spectrum of the  $s$ th sub-band of the  $m$ th ECG lead is defined as

$$B_s^m(k1, k2) = E[s^m(k1)s^m(k2)s^{*m}(k1+k2)] \quad (3)$$

where 'E' is the expectation operator and  $1 \leq k1 \leq N_s$ ,  $1 \leq k2 \leq N_s$ .  $N_s$  is the length of the  $s$ th sub-band. The analytic form of the CWSB is given by

$$B_s^m(k1, k2) = \tilde{B}_s^m(k1, k2) + j\overline{B}_s^m(k1, k2) \quad (4)$$

The magnitude of the CW bi-spectrum of the  $s$ th sub-band of the  $m$ th ECG lead is defined as

$$M_s^m(k1, k2) = \sqrt{[\tilde{B}_s^m(k1, k2)]^2 + [\overline{B}_s^m(k1, k2)]^2} \quad (5)$$

Similarly, the phase of the CW bi-spectrum in the  $s$ th sub-band of the  $m$ th ECG lead is defined by

$$\phi_s^m(k1, k2) = \tan^{-1} \left[ \frac{\tilde{B}_s^m(k1, k2)}{\overline{B}_s^m(k1, k2)} \right] \quad (6)$$

The lead V5 ECG signals for NSR and three pathological cases such as MI, BBB and CM are shown in Figs. 2a, f, k and p, respectively. It is noted that the shape and the beat to beat variations of the P-wave, the QRS-complex and the T-wave of ECG signals are different for BBB, CM and MI cases. The  $cA_6$ ,  $cD_6$ ,  $cD_5$  and  $cD_4$  sub-band signals (Signal reconstructed using the CW coefficients of each significant sub-band.) for NSR, MI, BBB and HMD cases are depicted in Figs. 2b–e, g–j, l–o and q–t, respectively. The bandwidth of an ECG signal spans the frequency range between 0.5 and 50 Hz [5]. The frequency contents of T-wave, P-wave and QRS-complex in ECG are [0.5–10 Hz], [5–30 Hz] and [8–50 Hz], respectively [25]. The frequency ranges of  $cA_6$ ,  $cD_6$ ,  $cD_5$  and  $cD_4$  sub-band signals are [0–7.81 Hz], [7.82–15.62 Hz], [15.63–31.24 Hz] and [31.25–62.5 Hz], respectively. The QRS-complex information is grossly captured in  $cD_6$ ,  $cD_5$  and  $cD_4$  sub-bands.

The information of ST-segment and the T-wave are observed in  $cA_6$  sub-band signal. Similarly, the P-wave information is captured using  $cA_6$  and  $cD_6$  sub-bands. From Fig. 2, it is observed that for BBB and HMD cases the QRS-complex information is appeared in  $cA_6$  sub-band signals. For MI case, the T-wave inversion is clearly observed in  $cA_6$  sub-band signal (as shown in Fig. 2g). The amplitude values of  $cD_4$  sub-band signals for BBB and HMD cases are less than those of healthy control (HC) and MI cases. The above observations infer that the CW coefficients of significant sub-band capture pathological variations due to different cardiac disorders. The CWSB magnitude and phase features evaluated from the CW coefficients of 12-lead ECG will be helpful for classification of MI, HMD and BBB pathology.

2.3. Magnitude and phase features of CWSB: The CW bi-spectrum of 12-lead ECG in significant sub-bands capture the diagnostic components. In this work, the magnitude and the phase features of CWSB for each ECG lead are evaluated. The magnitude feature is defined as the mean of the absolute value of the CWSB. The magnitude feature of CW bi-spectrum in the  $s$ th scale of the  $m$ th ECG lead is defined as

$$BM_s^m = \frac{1}{N_s^2} \sum_{k1=0}^{N_s} \sum_{k2=0}^{N_s} M_s^m(k1, k2) \quad (7)$$

where BM corresponds to the bi-spectrum magnitude. The phase features of CWSB such as the number of NP (NNP) angle and the number of positive phase (NPP) angle are evaluated. The algorithm for evaluation of NNP and NPP features of CW bi-spectrum in the  $s$ th sub-band is defined as follows.

**Algorithm:** Evaluation of CWSB phase features

**Input:** phase of the CW bi-spectrum of the  $s$ th sub-band of the  $m$ th lead:  $\phi_s^m(k1, k2)$ ,  $1 \leq k1 \leq N_s$  and  $1 \leq k2 \leq N_s$ .

**Output:** NNP and NPP features of the  $s$ th sub-band of the  $m$ th lead:  $NNP_s^m$ ,  $NPP_s^m$ .

**begin**

- The NPP angles of the  $s$ th sub-band of the  $m$ th lead are  $NPP_s^m = \text{count}(\phi_s^m(k1, k2) > 0)$ .
- The NNP angles of the  $s$ th sub-band of the  $m$ th lead are  $NNP_s^m = \text{count}(\phi_s^m(k1, k2) < 0)$ .

**end**

Figs. 3a–d show the magnitude contours of the CW bi-spectrum of  $cA_6$  sub-band for different cardiac ailments and NSR. Significant differences in the morphology of magnitude contours are observed for both NSR and pathological cases. The magnitude of CW bi-spectrum captures the third-order correlations of wavelet coefficients. The structure of CW bi-spectrum matrix at each scale is different for NSR and cardiac ailments. The BM, the NNP and the NPP features capture the changes in the CW bi-spectrum matrix of different sub-bands during pathology. The values of BM features for NSR, MI, BBB and HMD cases in  $cA_6$  sub-band are 0.7772, 0.2621, 2.8800 and 0.1905, respectively. Similar changes in the values of BM features are observed for NSR, MI, HMD and BBB cases in other sub-bands. In BBB and HMD pathologies, some part of the QRS-complex information is appeared in  $cA_6$  sub-band signal (as shown in Figs. 2l and q). The characteristics of  $cA_6$  sub-band signal for BBB and NSR cases are different. Owing to this reason, the BM feature for BBB case has higher value in  $cA_6$  sub-band than NSR, HMD and MI cases.

Figs. 3e–h depict the histogram of the phase of CW bi-spectrum in  $cA_6$  sub-band for NSR, BBB, HMD and MI cases. It is observed that the peaks of the histograms of the CWSB are different for

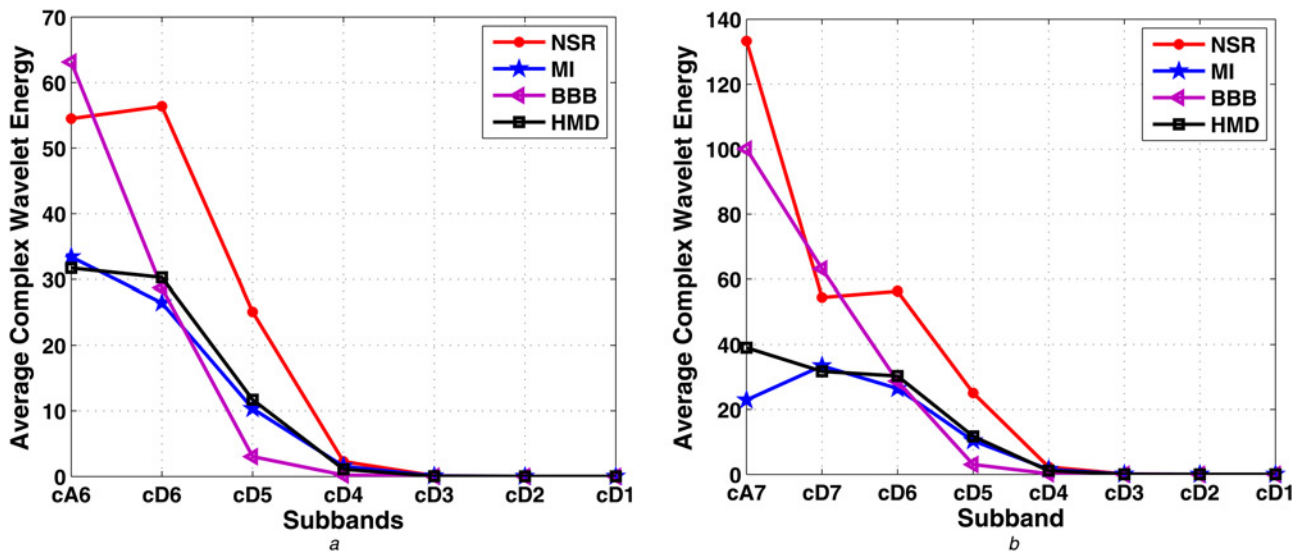


**Fig. 1** Variation of average CWE of all ECG leads  
 a Average CW energy of all leads in different sub-bands for six-level-based DTCWT decomposition of multilead ECG signals for NSR, MI, HMD and BBB  
 b Average CW energy of all leads in different sub-bands for seven-level-based DTCWT decomposition of multilead ECG signals for NSR, MI, HMD and BBB

cardiac ailments and NSR. The NNP and NPP features capture the variations in the phase of CWSB during pathology. The NNP values of CW bi-spectrum of  $cA_6$  sub-band for NSR, MI, BBB

and HMD cases are 2405, 1895, 2162 and 2337, respectively. Similarly, the NPP values are 1961, 2201, 1934 and 1759 for NSR, MI, BBB and HMD cases in  $cA_6$  sub-band. Similar

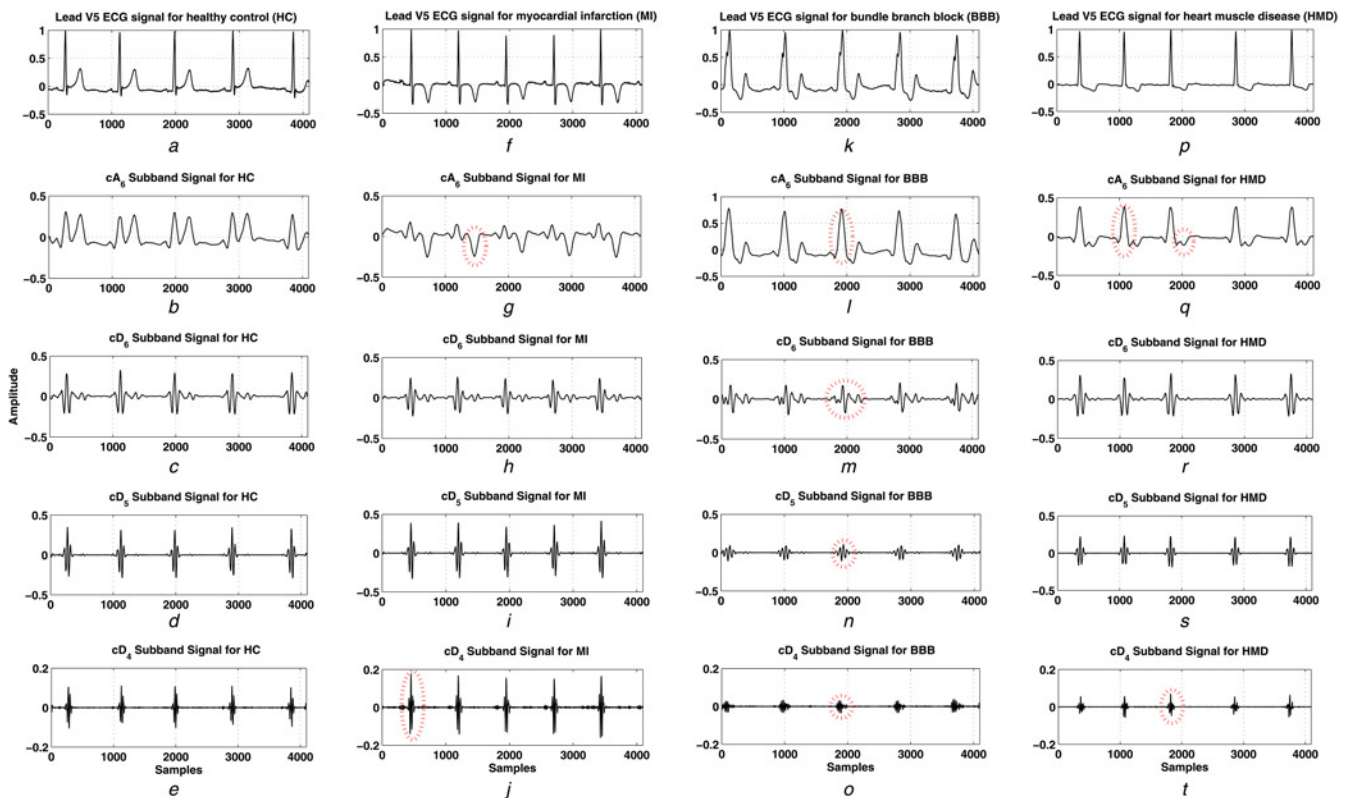


**Fig. 2** Lead V5 ECG signals for NSR and three pathological cases such as MI, BBB and CM  
 a Lead V5 ECG signal for HC  
 f Lead V5 ECG signal for MI  
 k Lead V5 ECG signal for BBB  
 p Lead V5 ECG signal for HMD (CM)  
 b-e  $cA_6$ ,  $cD_6$ ,  $cD_5$  and  $cD_4$  sub-band signals for HC  
 g-j  $cA_6$ ,  $cD_6$ ,  $cD_5$  and  $cD_4$  sub-band signals for MI  
 l-o  $cA_6$ ,  $cD_6$ ,  $cD_5$  and  $cD_4$  sub-band signals for BBB  
 q-t  $cA_6$ ,  $cD_6$ ,  $cD_5$  and  $cD_4$  sub-band signals for HMD

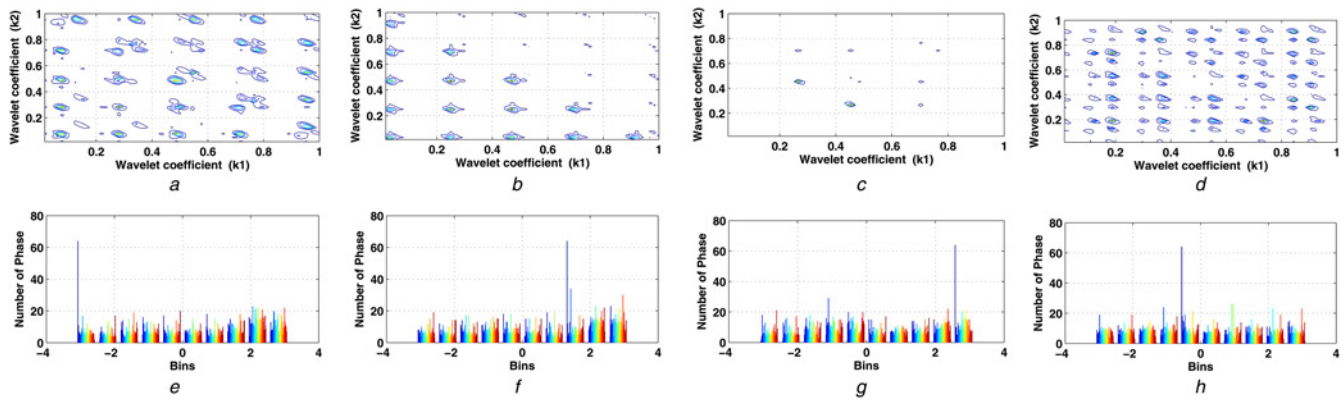


**Fig. 3** Magnitude contours of the CW bi-spectrum of  $cA_6$  sub-band for different cardiac ailments and NSR  
*a-d* Magnitude contour of the  $cA_6$  SB of NSR, BBB, HMD and MI  
*e-h* Histogram of the phase of  $cA_6$  SB of NSR, BBB, HMD and MI

changes in the NNP and NPP features of CWSB are also observed for  $cD_6$ ,  $cD_5$  and  $cD_4$  sub-bands. These variations in the BM, NNP and NPP values of CWSB can be used for detection and classification of cardiac disorders.

**3. Classification of cardiac ailments:** In this section, the proposed CWSB features of 12-lead ECG are used for classification of cardiac ailments. The flowchart of the classification method is shown in Fig. 4. It consists of 12-lead ECG data and preprocessing, evaluation of magnitude and phase features of CWSB, and classification using support vector machine (SVM) and extreme learning machine (ELM) classifiers.

**3.1. 12-Lead ECG data and preprocessing:** In this Letter, the 12-lead ECG datasets from a publicly available database (Physikalisch Technische Bundesanstalt (PTB) diagnostic database) is used for evaluation of the proposed method [26]. In this work, we have used 16, 16, 16 and 20 number 12-lead ECG datasets (lead I-V6) from NSR, MI, BBB and HMD (CM and hypertrophy (HT)) classes. The 12-lead ECG datasets from NSR and pathological cases are subjected to preprocessing. The preprocessing step consists of filtering of multilead ECG data and block-based

segmentation. For elimination of baseline wandering noise, a zero-phase Butterworth high-pass filter with cut-off frequency of 0.5 Hz is applied [16]. The high-frequency noise is filtered out based on the elimination of the CW coefficients of diagnostically irrelevant sub-bands [20]. The block-based segmentation of 12-lead ECG data is done using a window of size  $4096 \times 12$  [20].

**3.2. Feature selection and classification:** In this work, we have evaluated 48 magnitude features and 96 phase features from the CWSB of 12-lead ECG. A 144-dimensional (144D) CWSB feature vector is created by appending both magnitude and phase features. A feature selection technique is used to select important features from the 144D CWSB feature vector. This technique is called as symmetrical uncertainty (SU)-based feature selection [27]. Here, the SU scores of each CWSB feature is evaluated and the features which have higher value SU score are retained for classification. In this Letter, the SVM and the ELM classifiers are used to classify the CWSB features of 12-lead ECG into four classes such as NSR, BBB, HMD and MI. Here, we have used three kernel functions such as linear, polynomial and radial basis function (RBF) [28]. The performance of the SVM classifier using CWSB features are compared for these kernel functions. The parameters such as  $C = 0.005$ , the degree of the polynomial (Poly) kernel ( $c = 5$ ), the 'One against One' multiclass coding and the standard deviation of the RBF kernel ( $\sigma = 0.25$ ) are selected in this work. The ELM classifier uses random hidden nodes to map the input feature vector to a higher dimension space and the least-square method is used to evaluate the weight between the hidden layer and the output layer [29]. It requires less computation for evaluation of the training parameters and this model has been used for classification of different cardiac arrhythmia from ECG [30]. Here, for ELM classifier we have used 'sine', 'radbas' and 'sigmoid' activation functions. The regularisation parameter of ELM classifier is selected as ( $\gamma = 0.9$ ). The hold-out cross-validation and the  $K$ -fold cross-validation approaches are considered for selection of training and test instances of ELM and SVM classifiers [11]. For  $K$ -fold cross-validation case,  $K = 5, 6$  and  $7$  are considered. The optimal value of ' $K$ ' is selected based on the performance of ELM and SVM classifiers using the CWSB features of 12-lead ECG. The individual class accuracy (IA) and the overall accuracy (OA) metrics are used to quantify the performance of ELM and SVM classifiers. The IA and the OA are evaluated using the confusion matrix [31].

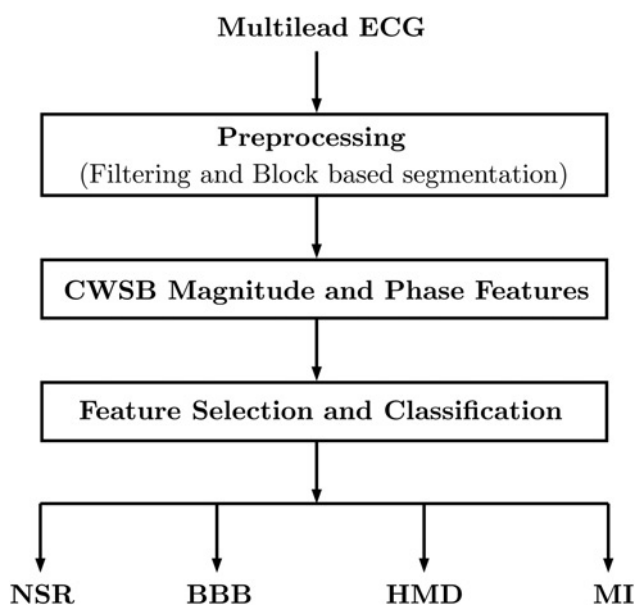


**Fig. 4** Detection and classification of cardiac ailments from CWSB features of multilead ECG

**4. Result and discussion:** In this section, the statistical analysis of CWSB features, and the performance of CWSB features using ELM and SVM classifiers are shown.

**Table 1** *p*-Values of selected CWSB features using ANOVA test

CWSB features	<i>p</i> -Value
$cA_6$ sub-band BM feature of lead I	<0.001
$cD_6$ sub-band BM feature of lead V1	<0.001
$cD_5$ sub-band BM feature of lead V3	<0.001
$cD_4$ sub-band BM feature of lead V5	<0.001
$cA_6$ sub-band NNP feature of lead I	<0.001
$cD_5$ sub-band NNP feature of lead V6	<0.001
$cA_6$ sub-band NNP feature of lead II	<0.001
$cD_5$ sub-band NNP feature of lead V4	<0.001
$cA_6$ sub-band NNP feature of lead I	<0.001
$cA_6$ sub-band NPP feature of lead I	0.0712
$cD_6$ sub-band NPP feature of lead V6	0.7083

**Table 2** OA value of classifiers for hold-out cross-validation

Training/test data percentage	Classifiers	OA, %
80% training and 20% testing	ELM	92.85
	SVM	98.39
70% training and 30% testing	ELM	95.07
	SVM	97.43

4.1. Statistical analysis of CWSB features: The mean and the standard deviation values of BM features of  $cA_6$ ,  $cD_6$ ,  $cD_5$  and  $cD_4$  sub-bands are different for cardiac ailments and NSR in each lead. For lead I, the mean values of BM features for (NSR, MI, HMD and BBB) in  $cA_6$ ,  $cD_6$ ,  $cD_5$  and  $cD_4$  sub-bands are (0.0304, 0.0206, 0.0412, 0.1134), (0.0757, 0.0425, 0.0557, 0.1142), (0.0763, 0.0880, 0.0476, 0.0702) and (0.0140, 0.0462, 0.0078, 0.0105), respectively. Similarly, for lead V6, the mean values of BM features for (NSR, MI, HMD and BBB) are (0.0130, 0.0092, 0.0286, 0.1073), (0.0714, 0.0871, 0.1050, 0.1305), (0.0779, 0.1094, 0.0710, 0.0648) and (0.0367, 0.1154, 0.0254, 0.0399) in  $cA_6$ ,  $cD_6$ ,  $cD_5$  and  $cD_4$  sub-bands. Similar variations in the mean and standard deviation values of the BM feature are observed in  $cA_6$ ,  $cD_6$ ,  $cD_5$  and  $cD_4$  sub-bands for other ECG leads. For  $cA_6$  sub-band of lead I, the mean values of NNP feature of CWSB for NSR, MI and BBB are 0.8370, 0.8616 and 0.8545, respectively. Similarly, the mean values of NPP feature of CWSB for NSR, BBB and HMD class are 0.7022, 0.7046 and 0.7057 in  $cA_6$  sub-band of lead V6. Similar changes in the mean and standard deviation values of NNP and NPP features of CWSB are observed for other ECG leads. These variations in the mean and the standard deviation values of BM, NNP and NPP features are due to the difference in the structure of CWSB matrix in pathology.

The statistical significance of CWSB magnitude and phase features are evaluated using analysis of variance (ANOVA) test [32]. It is observed that only 43 features out of 48 magnitude features

of CWSB have *p*-value <0.001 and these features are highly significant for detection of HMD, BBB and MI pathologies. It is also seen that all the NNP features of  $cA_6$  and  $cD_5$  sub-bands CW bi-spectrum have *p*-value lower than 0.001. The CW bi-spectrum phase features of  $cA_6$  and  $cD_5$  sub-bands capture the diagnostic information of multilead ECG. During pathology, the duration and the shape of the clinical components are different than the normal heart rhythm [1]. This maybe the reason for which the NNP features of CW bi-spectrum are statistically significant in  $cA_6$  and  $cD_5$  sub-bands. The *p*-values of the selected CWSB features are shown in Table 1. It is seen that out of 12 selected features, all the BM and NNP features have lower *p*-value. The *p*-value of selected NPP features are higher than 0.001. The above observations reveal that the CWSB features can capture the pathological changes of multilead ECG for detection of cardiac ailments.

4.2. Performance of SVM and ELM classifiers: In this section, the performance of SVM and ELM classifiers are shown using different combinations of CWSB features. The OA accuracy values of classifiers for hold-out cross-validation is shown in Table 2. Here, two hold-out cross-validation methods are considered for selection of training and test instances of ELM and SVM classifiers. In the first method, 70% of CWSB feature instances are used for training and the rest of 30% are considered for testing of both classifiers. Similarly, 80% of CWSB feature instances are used for training in the second method. It is observed that the SVM classifier have a higher accuracy value using 20% of CWSB feature instances.

For SVM and ELM classifiers, the IA of NSR, BBB, HMD and MI classes are evaluated along each fold and these values are shown in Table 3. It is observed that the SVM classifier has higher accuracy value for MI, HMD and BBB classes using  $cA_6$  and  $cD_6$  CWSB features. When  $cD_5$  and  $cD_4$  CWSB features are used, the accuracy value of ELM classifier is higher than the SVM classifier for BBB class. For ELM classifier, the performances of  $cA_6$  and  $cD_6$  CWSB features are higher than the  $cD_5$  and  $cD_4$  CWSB features. The SVM classifier shows better performance for each class using  $cD_5$  and  $cD_4$  CWSB features. The SVM classifier has higher IA values for BBB, MI and HMD classes using all CWSB features. The pathological variations in 12-lead ECG due to BBB, MI and HMD are effectively captured using proposed CWSB magnitude and phase features. This maybe the reason for better performance of ELM and SVM classifiers for MI, HMD and BBB classes. In 12-lead ECG, eight ECG leads (I, II, V1–V6) are directly recorded from the patient, whereas the remaining four leads (III, aVR, aVL and aVF) are derived from lead I and lead II. It is natural to get correlations in 12-lead ECG and these correlations are reflected in the CWSB feature matrix. In this Letter, the performances of classifiers are compared using the CWSB features of both 12-lead and 8-lead ECG signals. The OA values of ELM and SVM classifiers for 12-lead ECG and 8-lead ECG CWSB features are shown in Table 4. It is observed that the OA value of RBF kernel-based SVM classifier is 97.75% using 12-lead ECG CWSB features. Similarly, using 8-lead ECG, the OA value of SVM classifier is

**Table 3** Average IA values of ELM and SVM classifiers for BBB, HMD, MI and NSR classes

Features	Classifiers	IA (NSR), %	IA (MI), %	IA (HMD), %	IA (BBB), %
$cA_6 + cD_6$ CWSB features	ELM	94.02	96.47	91.30	88.08
$cA_6 + cD_6$ CWSB features	SVM	92.10	94.56	91.52	91.41
$cD_5 + cD_4$ CWSB features	ELM	86.15	93.76	95.00	68.17
$cD_5 + cD_4$ CWSB features	SVM	94.56	96.19	94.13	92.51
all CWSB features	ELM	95.93	98.37	97.39	92.79
all CWSB features	SVM	97.55	98.37	96.52	96.12
selected CWSB features	ELM	95.91	97.83	98.70	94.45
selected CWSB features	SVM	98.90	98.37	97.39	96.40

**Table 4** OA values of ELM and SVM classifiers using CWSB features of 8-lead ECG and 12-lead ECG

8-lead ECG			12-lead ECG		
Classifiers	Kernels	OA, %	Classifiers	Kernels	OA, %
ELM	sigmoid	84.51	ELM	sigmoid	88.11
ELM	radbas	92.67	ELM	radbas	95.05
ELM	sine	94.66	ELM	sine	96.08
SVM	linear	91.97	SVM	linear	94.54
SVM	polynomial	78.80	SVM	polynomial	85.86
SVM	RBF	95.63	SVM	RBF	97.75

95.63%. The performance of ELM classifier for 12-lead ECG CWSB features is higher than the 8-lead ECG CWSB features. The characteristics of lead III and lead aVF ECG signals are different for inferior MI and NSR [1]. These pathological changes can affect the CW bi-spectrum matrices of lead III and lead aVF in different sub-bands. This maybe the reason for which the higher OA values of ELM and SVM classifiers are observed using the CWSB features of 12-lead ECG.

The classes of cardiac ailments in the proposed method are different than the reported techniques. In this work, to verify the effectiveness of the proposed method, we have compared only the IA values of MI and HMD classes with existing 12-lead ECG-based cardiac arrhythmia detection approaches and it is shown in Table 5. In [9], Sun *et al.* have used the polynomial coefficients of ST-segments of 12-lead ECG as diagnostic features and different classifiers for detection of MI. In [10], the hermite coefficients of 12-lead ECG and the artificial neural network (ANN) are used for detection of MI. The method in [16] has used MEES features of multilead ECG for detection of MI. The principal component multivariate multiscale sample entropy (PMMSE) features have been used in [11] for classification of cardiac disorders. The detection of hypertrophic CM using the temporal and the morphological features of 12-lead ECG has been proposed in [14]. The proposed method show better performance for MI class than the techniques reported in [9–11, 15, 16]. The IA value of proposed CWSB features and the SVM classifier for HMD classes is higher than the performance of morphological features of 12-lead ECG. The method for detection of cardiac ailments using CWSB features is implemented in MATLAB 2010 with a desktop computer (4 GB random access memory and Intel i5 processor with 3.20 GHz). The simulation times for preprocessing and evaluation of CWSB features are 0.016 and 0.355 s, respectively. For SVM and ELM classifiers, the simulation times for testing of the CWSB feature vector of multilead ECG block are found to be 0.032 and 0.026 s, respectively. The above observations establish that the CWSB

**Table 5** Comparison of the proposed work with existing methods for 12-lead ECG signals

Features+classifier	IA (MI), %	IA (HMD), %
morphological features+ANN [15]	95	NU
polynomial coefficients+MIL [9]	91	NU
hermite coefficients+ANN [10]	83.4	NU
PMMSE features+LS-SVM [11]	93.95	89.16
morphological features+RF [14]	NU	90
MEES features+SVM [16]	96	NU
proposed multiscale PA features+fuzzy KNN [20]	94.31	80.90
proposed CWSB features+SVM	98.37	97.39

NU – not used.; MIL – multi instance learning; RF – random forest, LS – least square

features evaluated using HOCWA are useful for detection of various cardiac ailments from 12-lead ECG.

**5. Conclusion:** In this Letter, a new method is proposed for estimating diagnostic features from 12-lead ECG. The HOCWA of 12-lead ECG is used for evaluation of CWSB. The CWSB magnitude and phase features of 12-lead ECG at different scales are evaluated. The statistical significance of CWSB magnitude and phase features are shown. The SU score-based feature selection approach is used. The SVM and the ELM classifiers are used for detection and classification of cardiac ailments using the CWSB features and the selected features. The OA values of 97.17 and 97.75% are found using ELM and SVM classifiers. The accuracy values for MI and HMD classes using the proposed method are higher than the existing techniques based on 12-lead ECG. The important finding of this Letter is that the CWSB magnitude and phase features correctly capture the clinical components of multilead ECG and provide discriminative diagnostic information for detection of cardiac ailments. In future, new diagnostic features of 12-lead ECG and vectorcardiogram maybe required for detection and localisation of other cardiac ailments.

**6. Funding and declaration of interests:** Conflict of interest: none declared.

## 7 References

- [1] Goldberger A.L.: ‘Clinical electrocardiography: a simplified approach’ (Elsevier Health Sciences, Philadelphia, USA, 2012)
- [2] Thygesen K., Alpert J.S., Jaffe A.S., *ET AL.*: ‘Third universal definition of myocardial infarction’, *J. Am. Coll. Cardiol.*, 2012, **60**, (16), pp. 1581–1598
- [3] Drezner J.A., Ashley E., Baggish A.L., *ET AL.*: ‘Abnormal electrocardiographic findings in athletes: recognising changes suggestive of cardiomyopathy’, *Br. J. Sports Med.*, 2013, **47**, (3), pp. 137–152
- [4] Acharya U.R., Fujita H., Sudarshan V.K., *ET AL.*: ‘Automated detection and localization of myocardial infarction using electrocardiogram: a comparative study of different leads’, *Knowl.-Based Syst.*, 2016, **99**, pp. 146–156
- [5] Clifford G.D., Azuaje F., McSharry P.: ‘Advanced methods and tools for ECG data analysis’ (Artech House Inc., London, UK, 2006)
- [6] Acharya R., Krishnan S.M., Spaan J.A., *ET AL.*: ‘Advances in cardiac signal processing’ (Springer, Berlin, Heidelberg, Germany, 2007)
- [7] Martis R.J., Acharya U.R., Lim C.M., *ET AL.*: ‘Characterization of ECG beats from cardiac arrhythmia using discrete cosine transform in PCA framework’, *Knowl.-Based Syst.*, 2013, **45**, pp. 76–82
- [8] Banerjee S., Mitra M.: ‘Application of cross wavelet transform for ECG pattern analysis and classification’, *IEEE Trans. Instrum. Meas.*, 2014, **63**, (2), pp. 326–333
- [9] Sun L., Lu Y., Yang K., *ET AL.*: ‘ECG analysis using multiple instance learning for myocardial infarction detection’, *IEEE Trans. Biomed. Eng.*, 2012, **59**, (12), pp. 3348–3356
- [10] Haraldsson H., Edenbrandt L., Ohlsson M.: ‘Detecting acute myocardial infarction in the 12-lead ECG using hermite expansions and neural networks’, *Artif. Intell. Med.*, 2004, **32**, (2), pp. 127–136
- [11] Tripathy R., Sharma L., Dandapat S.: ‘A new way of quantifying diagnostic information from multilead electrocardiogram for cardiac disease classification’, *Healthc. Technol. Lett.*, 2014, **1**, (4), p. 98
- [12] Bogdanova I., Rincón F., Atienza D.: ‘A multi-lead ECG classification based on random projection features’. 2012 IEEE Int. Conf. on Acoustics, Speech and Signal Processing (ICASSP), 2012, pp. 625–628
- [13] Huang K., Zhang L.: ‘Cardiology knowledge free ECG feature extraction using generalized tensor rank one discriminant analysis’, *EURASIP J. Adv. Signal Process.*, 2014, **2014**, (1), pp. 1–15
- [14] Rahman Q.A., Tereshchenko L.G., Kongkatong M., *ET AL.*: ‘Utilizing ECG-based heartbeat classification for hypertrophic cardiomyopathy identification’, *IEEE Trans. NanoBiosci.*, 2015, **14**, (5), pp. 505–512
- [15] Hedén B., Öhlin H., Rittner R., *ET AL.*: ‘Acute myocardial infarction detected in the 12-lead ECG by artificial neural networks’, *Circulation*, 1997, **96**, (6), pp. 1798–1802
- [16] Sharma L., Tripathy R., Dandapat S.: ‘Multiscale energy and eigen-space approach to detection and localization of myocardial infarction’, *IEEE Trans. Biomed. Eng.*, 2015, **62**, (7), pp. 1827–1837

- [17] Selesnick I.W., Baraniuk R.G., Kingsbury N.G.: 'The dual-tree complex wavelet transform', *IEEE Signal Process. Mag.*, 2005, **22**, (6), pp. 123–151
- [18] Takla G., Loparo K.A., Nair B.: 'System for artifact detection and elimination in an electrocardiogram signal recorded from a patient monitor'. US Patent App. 12/116,235, 7 May 2008
- [19] Thomas M., Das M.K., Ari S.: 'Automatic ECG arrhythmia classification using dual tree complex wavelet based features', *AEU-Int. J. Electron. Commun.*, 2015, **69**, (4), pp. 715–721
- [20] Tripathy R., Dandapat S.: 'Detection of cardiac abnormalities from multilead ECG using multiscale phase alternation features', *J. Med. Syst.*, 2016, **40**, (6), pp. 1–9
- [21] Martis R.J., Acharya U.R., Prasad H., *ET AL.*: 'Application of higher order statistics for atrial arrhythmia classification', *Biomed. Signal Process. Control*, 2013, **8**, (6), pp. 888–900
- [22] Martis R.J., Acharya U.R., Mandana K., *ET AL.*: 'Cardiac decision making using higher order spectra', *Biomed. Signal Process. Control*, 2013, **8**, (2), pp. 193–203
- [23] Acharya U.R., Sudarshan V.K., Koh J.E., *ET AL.*: 'Application of higher order spectra for the characterization of coronary artery disease using electrocardiogram signals', *Biomed. Signal Process. Control*, 2017, **31**, pp. 31–43
- [24] Hadjileontiadis L.J.: 'EEG-based tonic cold pain characterization using wavelet higher order spectral features', *IEEE Trans. Biomed. Eng.*, 2015, **62**, (8), pp. 1981–1991
- [25] Tereshchenko L.G., Josephson M.E.: 'Frequency content and characteristics of ventricular conduction', *J. Electrocardiol.*, 2015, **48**, (6), pp. 933–937
- [26] Oeff M., Koch H., Boussejot R., *ET AL.*: 'The PTB diagnostic ECG database' (National Metrology Institute of Germany, Brandenburg, Germany, 2012). Available at <http://www.physionet.org/physiobank/database/ptbdb>
- [27] Huang C.-J., Yang D.-X., Chuang Y.-T.: 'Application of wrapper approach and composite classifier to the stock trend prediction', *Expert Syst. Appl.*, 2008, **34**, (4), pp. 2870–2878
- [28] Cristianini N., Shawe-Taylor J.: 'An introduction to support vector machines and other kernel-based learning methods' (Cambridge University Press, Cambridge, UK, 2000)
- [29] Huang G.-B., Zhou H., Ding X., *ET AL.*: 'Extreme learning machine for regression and multiclass classification', *IEEE Trans. Syst. Man Cybern. B, Cybern.*, 2012, **42**, (2), pp. 513–529
- [30] Karpagachelvi S., Arthanari M., Sivakumar M.: 'Classification of electrocardiogram signals with support vector machines and extreme learning machine', *Neural Comput. Appl.*, 2012, **21**, (6), pp. 1331–1339
- [31] Duda R.O., Hart P.E., Stork D.G.: 'Pattern classification' (John Wiley & Sons, USA, 2012)
- [32] Bland M.: 'An introduction to medical statistics' (OUP Oxford, London, UK, 2015)